# PRODUCTION OF AL- $B_4C$ FUNCTIONALLY GRADED MATERIAL BY POWDER METALLURGY METHOD

Aykut Canakci[1], Temel Varol[1], Ihsan Gokhan Zerin, Serdar Özkaya

[1]Department of Metallurgical and Materials Engineering, Karadeniz Technical University, Trabzon, Turkey aykut@ktu.edu.tr, tvarol@ktu.edu.tr

## ABSTRACT

The aim of this study is to examine the effects of the processing conditions on the final microstructure of Al-$B_4C$ functionally graded materials (FGMs). Al-$B_4C$ functionally graded material (FGM) having a compositional gradient from Al to $B_4C$ was obtained by powder metallurgy method with Al and $B_4C$ powders as starting materials. For this purpose laminar type of functionally graded Al-$B_4C$ with 1, 2 and 3 layers, which have different compositions, were produced. The functionally graded materials were analysed using a scanning electron microscopy (SEM). The microstructure, elemental distribution and microhardness variation of the sintered Al-$B_4C$ samples were investigated. The experimental results show that the distributions of structure properties strongly depend on the variation of microstructure. It is observed that hardness increases and ductility decreases with the increase of $B_4C$, which is attributed to the variation of the matrix phase from the metal to the ceramic. Morever, The results showed that laminar type is an effective method for Al-$B_4C$ functionally graded materials production.

**Keywords:** Functionally graded materials, Powder metallurgy, Boron carbide ($B_4C$)

## 1. INTRODUCTION

Functionally graded material (FGM) is a new concept in material design. FGMs with continuous changes of microstructures and properties across the material are expected to have low residual and thermal stresses and improved bonding strength between dissimilar materials and ceramic coatings. The unique characteristics in structure distribution makes FGM offer great promise in applications in many areas and the researches have been widely performed. It is well known that FGM performance depends mainly on the composition distribution. The composition distribution in FGMs can be tailored to specific requirements and properties of the constituent materials. For example, the structure of ceramic/metal FGMs is designed by considering the thermomechanical properties of the metal that has high mechanical strength and thermal conductivity of the ceramics that acts as a heat-resisting thermal shield. Therefore, ceramic/metal FGMs have received growing attention as prospective thermal barrier materials. A number of numerical analyses and experimental methods have been developed to evaluate the mechanical and thermal properties of FGMs [1-5].

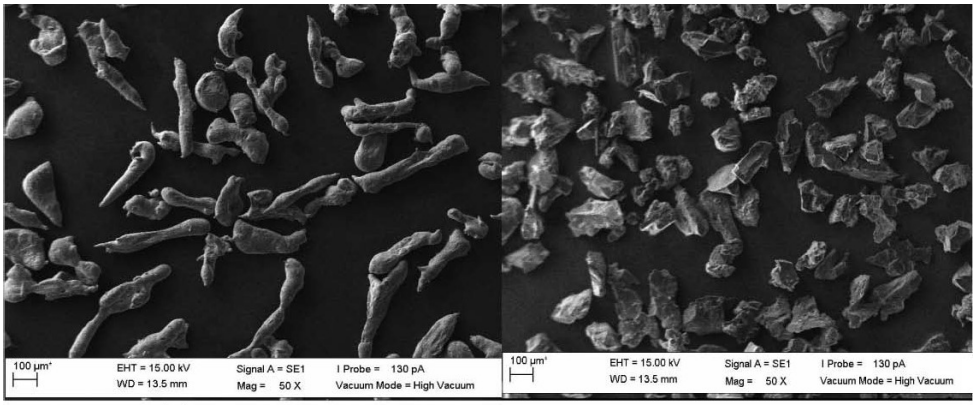
Various techniques have been employed to the fabrication of FGM, including physical and chemical vapor deposition, sintering, plasma spraying, electroplating and combustion synthesis. Powder metallurgical processing is one of the most viable routes for FGM, because the composition and microstructure as well as shape forming of FGM can be easily controlled in a wide range [2,6,7]. The powder metallurgy (PM) or ceramic technology route for processing of materials and engineering parts includes powder production, powder processing, forming operations and sintering or pressure assisted hot consolidation. Powders of many metals, alloys, compounds and ceramic materials with particle sizes ranging from nanometers to several hundred micrometers are available from industrial sources or may be produced by the methods developed over decades in the field of PM or ceramics. Since the material used to form the sintered part is dispersed into very small portions of individual powder particles nearly ideal conditions exist to build-up graded materials with varying chemistry or microstructure by using the particles as building blocks. Practical considerations towards an efficient process design suggest the use of powder mixtures with changing average particle size or composition during deposition of the material prior to the forming operation. It depends on the method applied for powder deposition whether a smooth change or a stepwise variation is obtained in the

green body. Since the consolidation of the green parts during sintering or hot pressing requires high temperatures at which diffusion processes are fast enough to enable densification, chemical reactions between particles of different compositions and the influence of particle size on the sintering behavior have to be taken into account for the final microstructure and dimensional control of the part. On the other hand thermodynamic factors acting during sintering may be used to create a gradient, e.g. during liquid-phase sintering [3,8].

The purpose of this research is to develop fundamental constitutional control technique of FGM by powder metallurgy, expecting to optimize FGM fabrication process and further improve its performance.The microstructure and the composition of the fabricated FGM by powder metallurgy were studied and the relative density and the Brinell hardness of each layer in the FGM were measured. The relationship between microstructure, composition, and some physical and mechanical properties were discussed.

## 2. EXPERIMENTAL PROCEDURES

Aluminium powders and $B_4C$ particles were used as raw materials to fabricate the FGMs. An average particle size of $B_4C$ particles used as reinforcement material and Al powders (Etial 7) used as matrix materials were 102μm and 113μm, respectively. Fig. 1(a) and (b) shows the morphologies of the as received Al matrix powders and $B_4C$particles [9].




(a) (b)

Fig. 1. Morphology of as-received powders: (a) Al alloy and (b) $Al_2O_3$ particles.

The Al matrix powders are ligamental in shape and the $B_4C$ particles are polygonal in shape. These powders are mechanically mixed and single-axis press, compressed raw samples produced at different pressures. The stacked layer were pressed at a pressure of 400 and 500 MPa. In this work, experiments on single-layer, two-layer and three-layer of Al-$B_4C$ FGM, as shown in Fig. 2 and Table1, are conducted [9].

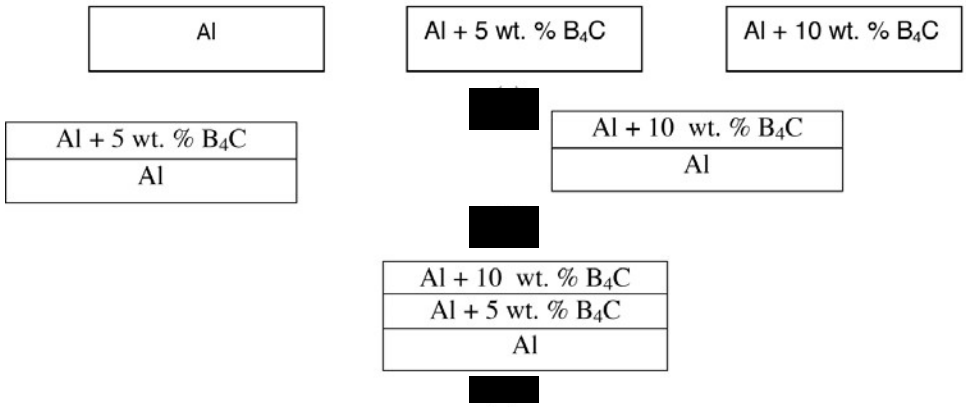



Fig. 2. The composition distribution model of Al-$B_4C$ FGMs. (a) Single-layer samples, (b) Two-layer samples, (c) Three-layer samples

Table 1.Configuration of FGMs.

| Coded Samples | Composition | Pressure (MPa) | Layer |
|---|---|---|---|
| $Al_{single}$(400) | 100 wt.% Al | 400 | Single |
| $Al_{single}$(500) | 100 wt. % Al | 500 | Single |
| Al-$5_{single}$ (400) | 95 wt.% Al + 5wt.% $B_4C$ | 400 | Single |
| Al-$5_{single}$ (500) | 95 wt.% Al + 5wt.% $B_4C$ | 500 | Single |
| Al-$10_{single}$(400) | 90 wt.% Al + 10wt.% $B_4C$ | 400 | Single |
| Al-$10_{single}$ (500) | 90 wt.% Al + 10wt.% $B_4C$ | 500 | Single |
| $(Al+Al-5)_{two}$(400) | 100 wt. % Al and 95 wt.% Al + 5wt.% $B_4C$ | 400 | Two |
| $(Al+Al-5)_{two}$(500) | 100 wt. % Al and 90 wt.% Al + 10wt.% $B_4C$ | 500 | Two |
| $(Al+Al-10)_{two}$(400) | 100 wt. % Al and 90 wt.% Al + 10wt.% $B_4C$ | 400 | Two |
| $(Al+Al-10)_{two}$(500) | 100 wt. % Al and 90 wt.% Al + 10wt.% $B_4C$ | 500 | Two |
| $(Al+Al-5+Al-10)_{three}$(400) | 100 wt. % Al , 95 wt.% Al + 5wt.% $B_4C$ and 90 wt.% Al + 10wt.% $B_4C$ | 400 | Three |
| $(Al+Al-5+Al-10)_{three}$(500) | 100 wt. % Al , 95 wt.% Al + 5wt.% $B_4C$ and 90 wt.% Al + 10wt.% $B_4C$ | 500 | Three |

The as-received Al alloy powder, the conventionally mixed (CM) powders were uniaxially cold pressed in a rectangular die with dimension of 30x30x20mm at 400 and 500MPa, with graphite as the die lubricant. The green compacts were sintered 600 °C for 3h under argon atmosphere. The sintered compacts were cooled to room temperature in the sintering furnace. The experimental density of the composite samples was measured using Archimede's method. In this technique, density is determined by measuring the difference between the samples weight in air and when it was suspended in distilled water at room temperature. The theoretical density was calculated using the mixture rule according to the volume fraction of the $B_4C$ particles. The porosities of FGMs were then evaluated from the difference between the expected and the observed density of each sample. To evaluate microstructure of produced composites the surface of samples were polished to achieve a rough surface of about 0.05µm. The morphologies and distribution of the $B_4C$ particles and the microstructures of the conventionally both mixed and the milled Al-$B_4C$ FGMs were analyzed on a Zeiss Evo LS10 scanning electron microscope (SEM) and a stereo microscopy.

The particle size distributions were determined using laser diffraction (Malvern, Model mastersizer Hydro 2000e), connected to a compute that models the volume size distribution, $D_{10}$, $D_{50}$, $D_{90}$ calculation automatically; three measurements were carried out for each sample. The hardness of the samples was measured using Brinell hardness method under a load of 31.25 kg held for 20s. Reported hardness values were the average of five measurements. With the variation of composition, the Al-$B_4C$ uniform compacts undergo very different shrinkage during densifications as shown in Fig. 3.

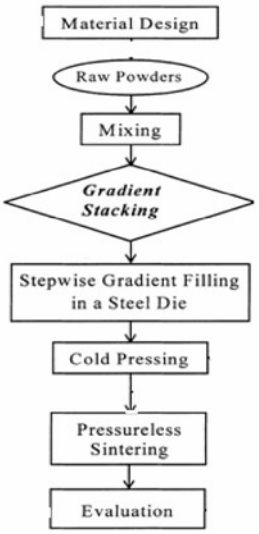
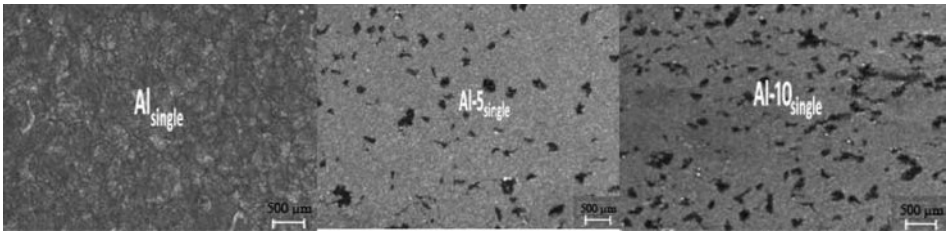



Fig. 3. Developing procedure of FGMs [9].

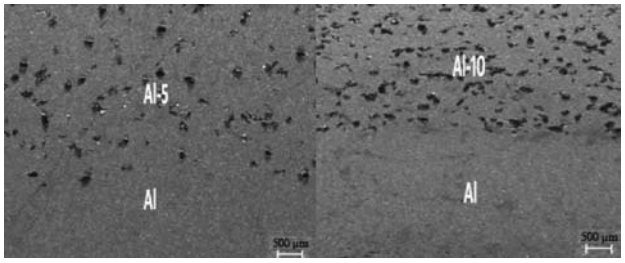
## 3. RESULTS AND DISCUSSIONS

### 3.1. Microstructure distribution

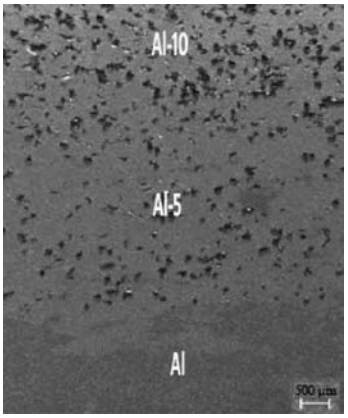
The optical and SEM images of the cross-section of the prepared FGM component are shown in Fig. 4 and Fig. 5, respectively.




(a)

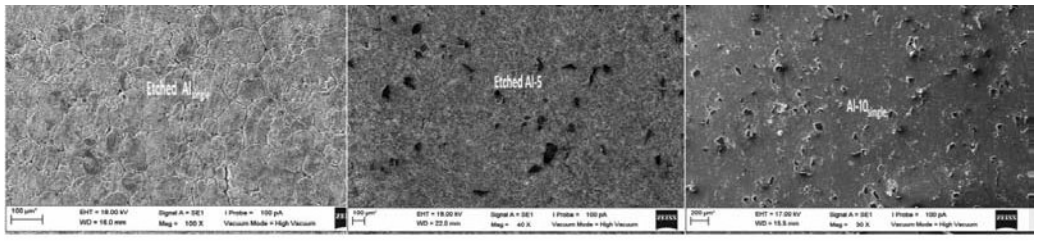



(b)

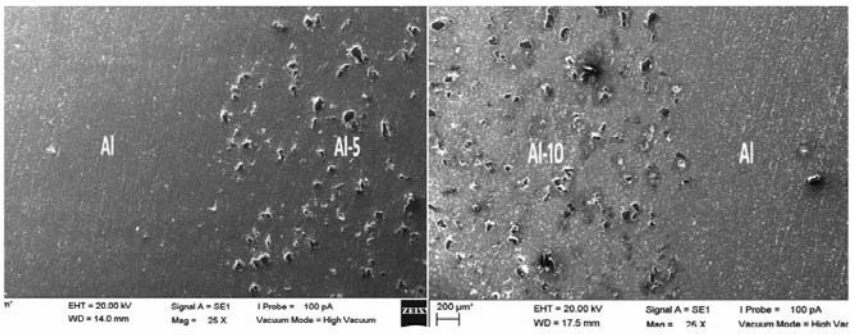



(c)

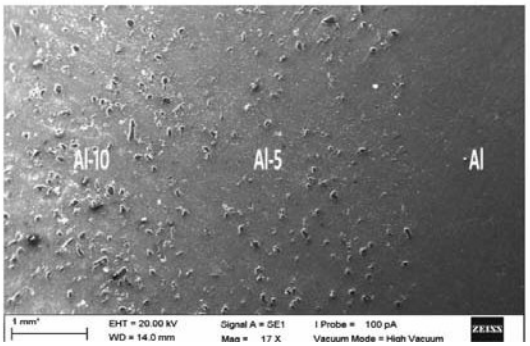
Fig. 4. Optical micrographs of different Al-$B_4C$ FGM fabricated by powder metallurgy (pressed at 500MPa). (a) Single-layer samples, (b) Two-layer samples, and (c) Three-layer sample.




(a)




(b)




(c)

Fig. 5. Scanning electron microscopy micrographs at different positions in FGMs. (a) Single-layer samples (pressed at 500MPa), (b) Two-layer samples (pressed at 400MPa), and (c) Three-layer sample (pressed at 400MPa)

It can be seen that the microstructure of the sample takes on a compositional gradient change along the thickness direction. The layer boundaries were observed clearly, which indicates that the structures of the FGMs were macroscopically heterogeneous due to the graded distribution of the composition. There aren't delaminations or defects at the interlayer boundaries. In the images, it is noted that the light phase in the FGMs is Al and the dark phase is $B_4C$, which is seen particularly clearly in the SEM image (Fig. 4). The microstructure of the sintered Al-$B_4C$ FGMs is presented in Fig. 5, where the gray and dark phases are Al and $B_4C$, respectively. These images show a good gradual compositional variation in the FGMs.

The obvious macroscopic interfaces are not observed even on the interfaces between different layers where the material composition jumps. Fig. 5 shows a typical variation of the microstructure in the FGMs. The varying microstructure is characterized by the gradual variation of the matrix phase from the metal to the ceramic with the increase of $B_4C$. In the metal-rich side, the ceramic particles are dispersed in the metal matrix. With the increase of $B_4C$, the clusters of the ceramic are formed and their further growths result in the formation of a network structure. Then, the network of the metal is gradually diminished and turns into the isolated metal particle dispersed in the ceramic matrix in the ceramic-rich side.

### 3.2. Some physical properties of FGMs

The graded change of the chemical compositions and microstructure in FGM leads to a continuous distribution of the properties. As shown in Fig. 6, 7 and Table 2, the density of theoretical, green and sintered and porosities of the FGMs according to the weight fractions of B4C particles. Al-$B_4C$ system show various graded distributions corresponding to constitutional change. Fig. 6, 7 and Table 2 show that density of green and sintered samples decreases with increasing $B_4C$ content. The graphs of green and sintered densities of the FGMs according to the weight fractions of $B_4C$ particles are shown in Figs. 6 and 7, respectively.

Table 2. Physical properties of FGMs [9].

| Coded samples | Theoretical density (g $cm^{-3}$) | Green density (g cm-3) | Sintered density (g cm-3) | Green porosity (%) | Sintered porosity (%) |
|---|---|---|---|---|---|
| $Al_{single}$(400) | 2.70 | 2.52 | 2.60 | 6.54 | 5.19 |
| $Al_{single}$(500) | 2.70 | 2.60 | 2.61 | 3.70 | 3.34 |
| Al-$5_{single}$ (400) | 2.69 | 2.51 | 2.51 | 6.74 | 6.58 |
| Al-$5_{single}$ (500) | 2.69 | 2.59 | 2.60 | 3.82 | 3.50 |
| Al-$10_{single}$(400) | 2.68 | 2.49 | 2.50 | 7.12 | 6.86 |
| Al-$10_{single}$ (500) | 2.68 | 2.57 | 2.58 | 4.27 | 3.69 |
| (Al+Al-5)$_{two}$(400) | 2.70 | 2.52 | 2.52 | 6.63 | 6.38 |
| (Al+Al-5)$_{two}$(500) | 2.70 | 2.59 | 2.60 | 3.75 | 3.42 |
| (Al+Al-10)$_{two}$(400) | 2.69 | 2.51 | 2.51 | 6.88 | 6.58 |
| (Al+Al-10)$_{two}$(500) | 2.69 | 2.59 | 2.60 | 3.84 | 3.49 |
| (Al+Al-5+Al-10)$_{three}$(400) | 2.69 | 2.50 | 2.51 | 7.09 | 6.72 |
| (Al+Al-5+Al-10)$_{three}$(500) | 2.69 | 2.59 | 2.59 | 4.20 | 3.75 |

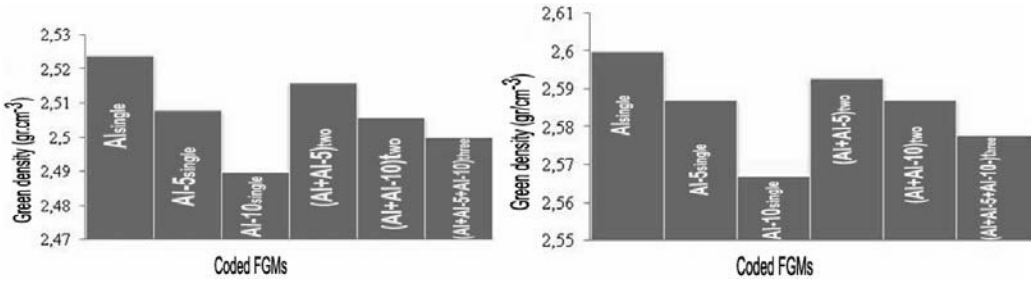



Fig. 6. The green densities of FGMs for different pressing pressure.(a) at 400MPa, (b) at 500MPa.

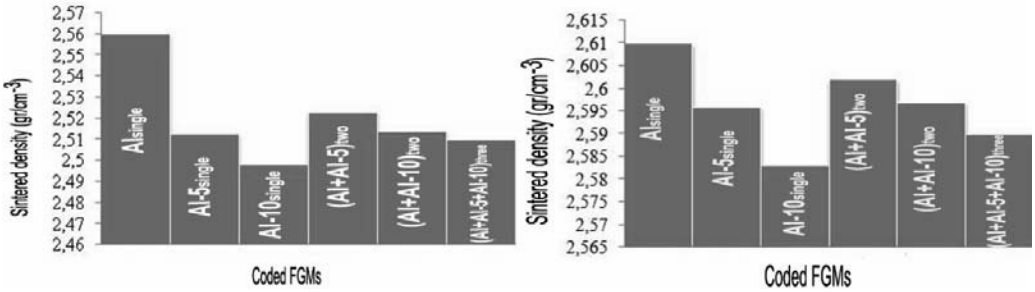



Fig. 7. The sintered densities of FGMs for different pressing pressure. (a) at 400MPa, (b) at 500MPa.

Table 3 shows that some theoretical density values of the FGMs decrease (as expected from the rule of mixtures). Although a decrease was also seen in the experimental densities (green and sintered density values), the value are lower than those theoretical ones. The density measurements showed that FGMs contain some porosity, and the amount of porosity in the green and sintered of FGMs increased with the increasing weight fraction of the particles (Fig. 8 and 9), as observed in the previous investigations [10-17].

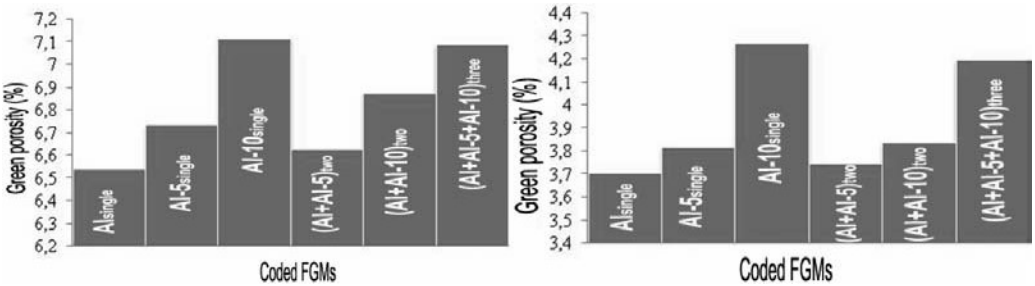



Fig. 8. The green porosities of FGMs for different pressing pressure.(a) at 400MPa, (b) at 500MPa.

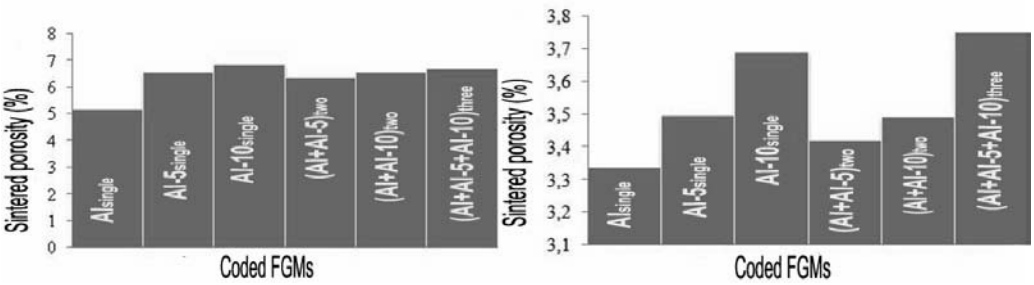



Fig. 9. The sintered porosities of FGMs for different pressing pressure.(a) at 400MPa, (b) at 500MPa.

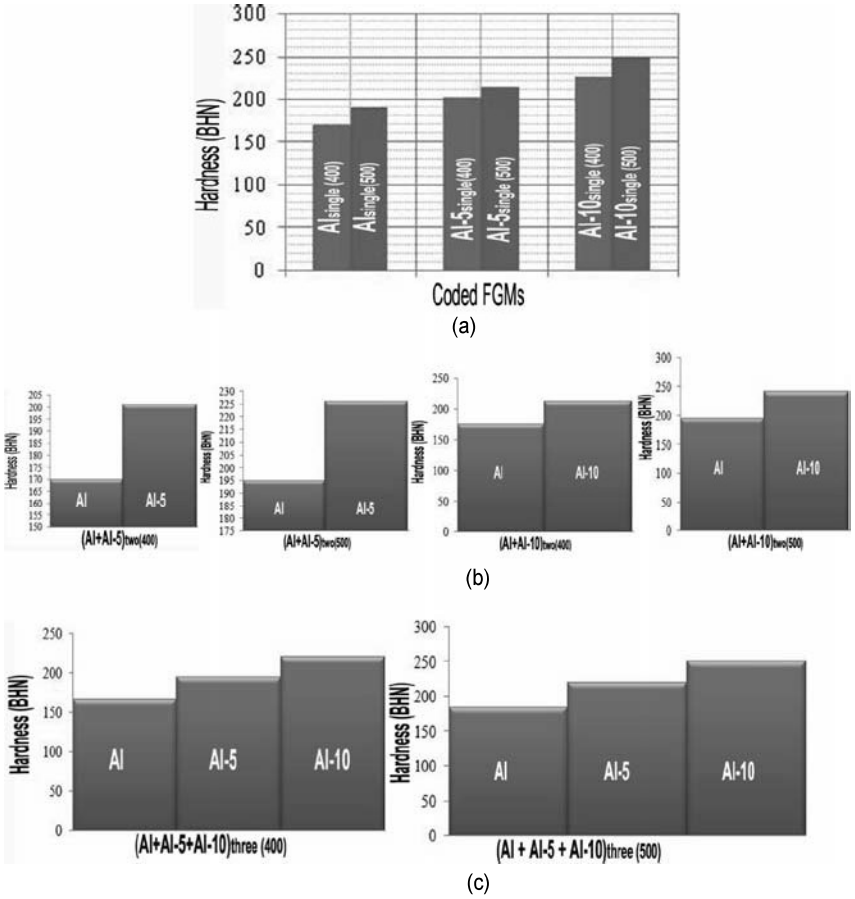
### 3.3. Hardness of FGMs

The influence of the varying microstructure on the hardness of the FGM sample is obvious, as shown in Fig. 10. As the content of $B_4C$ increases from 0% to 10%, the slope of the hardness curve changes and the hardness increases substantially. This is mainly caused by the gradual variation of the microstructure inthe FGMs. In these layers, the matrix phase varies from the softmetal to the hard ceramic, as shown in Fig. 4 and 5. The Brinell hardness of the FGMs and single-layers were given in Table 3. The relation between the $B_4C$ particle content and the hardness of the FGMs were plotted in Fig. 10. It was seen from Fig. 10 that the hardness of the FGMs increased with increasing particle weight fraction. As compared to the $Al_{single}$ matrix alloy, the hardness of the FGMs was found to be greater, and addition of $B_4C$ particles increase the hardness of the Al alloy [11,18].

Table 3. The hardness properties of FGMs.

| Coded samples | Brinell Hardness (BHN) |
|---|---|
| $Al_{single}$(400) | 170 |
| $Al_{single}$(500) | 189 |
| Al-$5_{single}$ (400) | 201 |
| Al-$5_{single}$ (500) | 213 |
| Al-$10_{single}$(400) | 226 |
| Al-$10_{single}$ (500) | 250 |
| (Al+Al-5)$_{two}$(400) | 170-201 |
| (Al+Al-5)$_{two}$(500) | 195-226 |
| (Al+Al-10)$_{two}$(400) | 175-213 |
| (Al+Al-10)$_{two}$(500) | 195-241 |
| (Al+Al-5+Al-10)$_{three}$(400) | 166-195-220 |
| (Al+Al-5+Al-10)$_{three}$(500) | 185-220-250 |

An increase in the hardness of the Al-$B_4C$ FGM with increasing weight fractions of $B_4C$ from the matrix to $B_4C$ graded regions, for both the FGM fabricated at 400 and 500MPa, respectively (Table 3, Fig. 10), as observed in the previous investigations [19,20].




(a)

(b)

(c)

Fig. 10. The Brinell hardness of FGMs.(a) Single-layer samples, (b) Two-layer samples, (c) Three-layer sample.

## 4. Conclusions

Single, two and three staged Al-$B_4C$ FGMs had been successfully fabricated by powder metallurgy technique. The relative density of the FGM was more than 93%. The relative density of the three stage FGM (500Mpa) was more than 95%. Microstructure analysis showed that a good graded composition of FGM had been obtained. The $B_4C$ particles were well embedded into the matrix by solid state sintering. The present work provides a effective approach to fabricating ceramic–metal FGM by powder metallurgy technical for different applications.

1. Al-$B_4C$ functionally graded material (FGM) has been successfully developed by the powder metallurgical process
2. Green and sintered density values increases with increasing pressure.
3. Green and sintered density values decreases with increasing $B_4C$ content.
4. Hardness of FGMs increases with the increasing $B_4C$ content.

## Acknowledgement

The authors are grateful to Karadeniz Technical University Research Fund for the financial supporting of this research work (No: 2007.112.10.2).

## References

1. Gang Jin, Makoto Takeuchi, Sawao Honda, Tadahiro Nishikawa, Hideo Awaji, Materials Chemistry and Physics 89 (2005) 238–243
2. Jingchuan Zhua, Zhonghong Lai , Zhongda Yin, Jaeho Jeon, Sooyoung Lee, Materials Chemistry and Physics 68 (2001) 130–135
3. B. Kieback, A. Neubrand , H. Riedel, Materials Science and Engineering A362 (2003) 81–105
4. Xin Jin, LinzhiWu, Yuguo Sun, Licheng Guo, Materials Science and Engineering A 509 (2009) 63–68
5. S. Lopez-Esteban, J.F. Bartolome , C. Pecharroman, J.S. Moya, Journal of the European Ceramic Society 22 (2002) 2799–2804
6. Zhang-Jian Zhou, Juan Du, Shu-Xiang Song, Zhi-Hong Zhong, Chang-Chun Ge, Journal of Alloys and Compounds 428 (2007) 146–150
7. Zeming He, J. Ma, G.E.B. Tan, Journal of Alloys and Compounds 486 (2009) 815–818
8. Li Sun, Basak Oguz, Patrick Kwon, Powder Technology 195 (2009) 227–234.
9. I.G. Zerin, S. Ozkaya, Karadeniz Technical University, Department of Metallurgical and Materials Engineering, Trabzon, Turkey, Graduation Thesis, 38 pages, 2011.
10. Manumanth GS, Iron GA (1993) J Mater Sci 28:2459. doi: 10.1007/BFO1151680
11. Kök M (2005) J Mater Process Technol 161:381
12. Kök M (2006) Composites A 37:457
13. Ghost PK, Ray S (1988) AFS Trans 775–782:88
14. Akhlaghi F, Lajervardi A, Maghanaki HM (2004) J Mater Process Technol 155–156:1874
15. McCoy OW and Franklin EW (1988) In: Fishman SG, Dhingra AK (eds) Cast reinforced metal composites. Chicago, USA, p 77
16. Ray S (1988) In: Fishman SG, Dhingra AK (eds) Proceedings of the survey on fabrication methods of cast reinforced metal composites. ASM/TMS, p 77
17. Cöcen U, Önel K (1996) Mater Sci Eng A 221:187
18. Purazrang K, Abachi P, Kainer KU (1994) Composites A 25(4):296
19. Rao AG, Mohape M, Kathar VA, Gowtam DS, Deshmukh VP and Shah AK (2010) Materials and Manufacturing Processes, 25: 572–576.
20. Lin CY, Bathias C, McShane HB and Rawlings RD (1999) Powder Metallurgy 42(1): 29-33.